

Review on ionization and quenching mechanisms of Trichel pulse

Anbang Sun(孙安邦), Xing Zhang(张幸), Yulin Guo(郭雨林), Yanliang He(何彦良), Guanjun Zhang(张冠军)
Citation: Chin. Phys. B, 2021, 30 (**5**): 055207. DOI: 10.1088/1674-1056/abd75d
Journal homepage: http://cpb.iphy.ac.cn; http://iopscience.iop.org/cpb

What follows is a list of articles you may be interested in

Enhancement of corona discharge induced wind generation with carbon nanotube and titanium dioxide decoration

Jianchun Ye(叶建春), Jun Li(李俊), Xiaohong Chen(陈晓红), Sumei Huang(黄素梅), Wei Ou-Yang(欧阳威)
Chin. Phys. B, 2019, 28 (**9**): 095202. DOI: 10.1088/1674-1056/ab33ed

Characteristics and underlying physics of ionic wind in dc corona discharge under different polarities

Tongkai Zhang(张桐恺), Yu Zhang(张宇), Qizheng Ji(季启政), Ben Li(李犇), Jiting Ouyang(欧阳吉庭)
Chin. Phys. B, 2019, 28 (**7**): 075202. DOI: 10.1088/1674-1056/28/7/075202

Numerical simulation of a direct current glow discharge in atmospheric pressure helium

Zeng-Qian Yin(尹增谦), Yan Wang(汪岩), Pan-Pan Zhang(张盼盼), Qi Zhang(张琦), Xue-Chen Li(李雪辰)
Chin. Phys. B, 2016, 25 (**12**): 125203. DOI: 10.1088/1674-1056/25/12/125203

Nitriding molybdenum： Effects of duration and fill gas pressure when using 100-Hz pulse DC discharge technique

U. Ikhlaq, R. Ahmad, M. Shafiq, S. Saleem, M. S. Shah, T. Hussain, I. A. Khan, K. Abbas, M. S. Abbas
Chin. Phys. B, 2014, 23 (**10**): 105203. DOI: 10.1088/1674-1056/23/10/105203

Investigation on the shockwave induced by surface arc plasma in quiescent air

Jin Di, Li Ying-Hong, Jia Min, Li Fan-Yu, Cui Wei, Sun Quan, Zhang Bai-Ling, Li Jun
Chin. Phys. B, 2014, 23 (**3**): 035201. DOI: 10.1088/1674-1056/23/3/035201

REVIEW

Review on ionization and quenching mechanisms of Trichel pulse*

Anbang Sun(孙安邦)†, Xing Zhang(张幸), Yulin Guo(郭雨林), Yanliang He(何彦良), and Guanjun Zhang(张冠军)

State Key Laboratory of Electrical Insulation and Power Equipment, School of Electrical Engineering, Xi'an Jiaotong University, Xi'an 710049, *China*

(Received 28 October 2020; revised manuscript received 26 December 2020; accepted manuscript online 30 December 2020)

Trichel pulse is a kind of pulsed mode in negative DC corona discharge, which has attracted significant attention because of its considerable applications in industry. Over eighty years, plenty of effort including simulations and experiments has been spent to reveal the ionization and quenching mechanisms of Trichel pulse. By revisiting and summarizing the basic characteristics and well-accepted ionization and quenching mechanisms, this review provides a basic understanding and the current status of Trichel pulse.

Keywords: Trichel pulse, negative corona discharge, DC discharge

PACS: 52.80.Hc, 51.50.+v, 52.80.–s **DOI:** 10.1088/1674-1056/abd75d

1. Introduction

Corona discharge is a kind of partial discharge in a sharply nonuniform electric field, where the electric field near large-curvature electrodes is much stronger than the other places.[1] It is an important and interesting topic in the industrial field, for example, in a power system, corona discharge can induce power loss, audible noise, electromagnetic radiation, and chemical corrosion,[2,3] which are undesirable. On the other hand, corona discharge has many beneficial applications in electrostatic precipitation, surface treatment, gas detection, biomedicine, generating charged aerosols, *etc*.[4–14] When applying direct current (DC) voltage and only one electrode generating a stronger electric field (unipolar corona), we can name it positive or negative corona discharge according to the polarity of the active electrode.[15] The negative corona discharge modes include pulsed mode, pulseless (glow) mode.[11,16] We will focus on the pulsed mode of negative DC corona discharge, especially Trichel pulse, in this review.

Traditionally, Trichel pulse, named and first reported by Trichel in 1938,[17] is a kind of pulsed mode of negative DC corona discharge in electronegative gases with a pulsating current under an appropriate negative voltage region. Lots of effort has been spent to reveal the underlying mechanisms that can lead Trichel pulse to generate and quench in a short time. The leading edge of Trichel can be as short as several nanoseconds, which has been explained by some mechanisms, such as successive or parallel electron avalanches fed by photoemission,[18–21] photoemission followed by positive ion-induced secondary electron emission (ISEE),[22,23] field emission,[24–26] a cathode-directed streamer mechanism.[27,29] However, a comprehensive theory of the leading edge has not been achieved yet, and the mechanism mentioned before is inconsistent with each other to some degree. On the other hand, quenching and regenerating of regular pulses are dominated by negative ions in electronegative gases, which is generally well accepted.[30–38] However, the pulsed mode has been reported in non-electronegative gases[40–45] which challenges the role of negative ions. In this review, we summarize the pulsed mode in non-electronegative gases (whether this mode can be called as Trichel pulse is still not conclusive) since we can get a comprehensive understanding of quenching mechanism through the comparison.

The paper is organized as follows. In Section 2, the basic optical and electrical characteristics of Trichel pulse are briefly introduced. Then, we highlight and analyze the current status of possible ionization and quenching mechanisms of Trichel pulse respectively that are available in published literatures, combining with our understanding. Finally, conclusions and outlooks are proposed briefly.

2. Basic characteristics of Trichel pulse

2.1. Optical characteristics

Usually, when a Trichel pulse is generated, a purple luminous region appears near the needle, as shown in Fig. 1(a).[46] With the current increase, it generally reaches the anode as shown in Fig. 1(b).[47] When reduced the pressure to some extent, the luminous area shows all the aspects of a classical glow discharge, including a dark cathode fall, a bright negative glow, a Faraday dark space, and a positive column as shown in Fig. 1(c).[15,17,18] Moreover, some researchers have found the ring-like Trichel pulse phenomenon in both experiments and simulations,[35,48,50] as shown in Fig. 1(d). And some of them

*Project supported by the National Natural Science Foundation of China (Grant No. 51777164) and the Fundamental Research Funds for the Central Universities, China (Grant Nos. xtr042019009 and PY3A083).

†Corresponding author. E-mail: anbang.sun@xjtu.edu.cn

© 2021 Chinese Physical Society and IOP Publishing Ltd

attributed this phenomenon to the field distortion caused by negative space charges. By using a microscope, Gallo *et al.*[37] discovered an extremely narrow "bright ionization channel", which expands from the cathode tip to the usual corona cone configuration, as shown in Fig. 1(e). The ionization channel wobbles around the tip erratically.

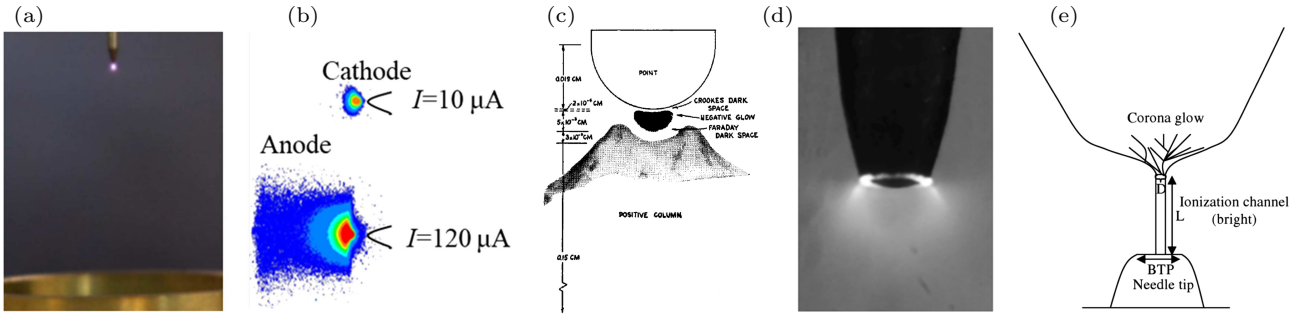


Fig. 1. The luminous area of Trichel pulse, (a) CMOS image,[46] (b) time-averaged CCD images, reproduced from Ref. [47], (c) schematic diagram at low pressure,[18] (d) ring-like Trichel pulse phenomenon,[49] (e) Trichel pulse with extremely narrow "bright ionization channel".[37]

2.2. Dynamic current and voltage

When Trichel pulse appears, the voltage keeps constant, while the current follows in a manner of very regular pulses. However, the first pulse is usually stronger than the following regular ones, since it is generated in a negative charge-free space. For the following pulses, negative ions accumulate and suppress the electric field leading to weaker ionization and smaller magnitude pulses, which is well explained by simulations.[31–33,35] When focusing on a single pulse, the leading edge is as short as several nanoseconds (especially at high pressure) and a stepped leading edge may be investigated.[23,28] The mechanisms of this fast leading edge will be discussed in the next section.

2.3. Time-averaged current and voltage

The well-known Townsend relation,[51] which was derived for a DC corona discharge under a wire-cylinder geometry, is also used for Trichel pulse under point-to-plane geometry,

$$I = k_{\mathrm{T}} V_{\mathrm{a}} \left(V_{\mathrm{a}} - V_0\right), \tag{1}$$

where I is the time-averaged current, k_{T} is a coefficient related to the needle electrode radius, particle mobility, and other geometrical factors, V_{a} is the applied voltage, V_0 is the corona onset voltage. Based on that, the relationship between time-averaged current and applied voltage has been summarized by many researchers, which can be categorized into two types. Type I is $I \propto V_{\mathrm{a}}(V_{\mathrm{a}} - V_0)$[30,52] and type II is $I \propto (V_{\mathrm{a}} - V_0)^2$.[53] The two types can be distinguished by checking the linear dependencies on a plot, $I/V_{\mathrm{a}} - V_{\mathrm{a}}$ for type I, and $I^{0.5} - V_{\mathrm{a}}$ for type II. Moreover, some researchers have found that the exponent of Type II could be other values which is determined by the data fitting.[54,55]

2.4. Frequency characteristics

The Trichel pulse frequency is usually from kHz to MHz. For given electrodes, the relation between frequency and time-averaged current (f–I) is summarized by Lama *et al.*[30]

$$f = \frac{1}{Q} I, \tag{2}$$

where Q is the charge per pulse, which keeps constant and is independent of I. While Amin[20] investigated that with I further increasing, Q would decrease to some degree.

Then, the relation between frequency and applied voltage (f–V_{a}) can be derived from the relations of f–I combined with I–V_{a}. So like I–V_{a}, two types of f–V_{a} exist, which have been verified by experiments. Lama *et al.*[30] summarized one type of f–V_{a} with considering different electrodes from their experiments,

$$f = k_{\mathrm{c}} V_{\mathrm{a}} \left(V_{\mathrm{a}} - V_0\right) / (rS^2), \tag{3}$$

where k_{c} is a constant, r is needle tip radius, S is the point-to-plane spacing. On the other hand, He *et al.*[55,56] proposed another type of f–V_{a} based on their experimental observation,

$$f = k_v \left(V_{\mathrm{a}} - V_0\right)^2, \tag{4}$$

where k_v is a constant for given electrodes.

3. Ionization mechanisms of Trichel pulse

The mechanisms involving the rise time of the leading edge which is on the order of nanosecond have attracted lots of attention and are one of the most important research fields in Trichel pulse. In Townsend theory, electron emission processes are essential to keep a self-sustained discharge. If there is no electron released from the cathode continuously, avalanches will move away from the cathode and no sustained discharge can form. Various electron emission mechanisms such as ISEE, photoemission, and field emission have been proposed to explain the fast leading edge. Meanwhile, some researchers used a cathode-directed streamer mechanism instead of feedback mechanisms to explain the fast leading edge, in which the effect of space charge was emphasized. Additionally, as photoionization is an important mechanism in the

evolution of streamers, its effect on Trichel pulse has been discussed through simulation. In this section, we will summarize some mechanisms from the literature that are relatively well accepted, and analyze the applicability of different mechanisms.

3.1. Cathode secondary electron emission

Usually, the emission of secondary electrons on cathode can be caused by photons or so-called photoemission (γ_p), by positive ions (γ_i), and by excited atoms (γ_e),[1] among which the first two mechanisms have been systematically investigated in the field of Trichel pulse.

3.1.1. Photoemission

Photoemission is caused by the photoelectric effect from the surface. With the avalanches development, the photons and positive ions are generated in the head of avalanches. Since the photons move much faster and reach the cathode much earlier than positive ions in the gas, photoemission can be responsible for the very initial stage of Trichel pulse. Loeb and Amin *et al.*[19,20] put forward that successive electron avalanches fed by photoemission could make Trichel pulse build up on the order of 10^{-8} s. Then this theory was extended by Alexandrov[21] considering parallel avalanches linked by photoemission leading to much faster rise time. Later, Morrow[22] considered photoemission in his fluid model to simulate the first Trichel pulse in oxygen at 6.67 kPa, which is the first simulation model of Trichel pulse. Then he[23] further explained the stepped leading edge phenomenon on the model, which means two rising processes contained in a leading edge. As shown in Fig. 2, the first rising process is caused by photoemission. Later, Černák[28] experimentally revealed that a graphite-coated cathode (low γ_p) can reduce the first step while a CuI-coated cathode (high γ_p) has the opposite effect, which is consistent with Morrow's theory to some extent.

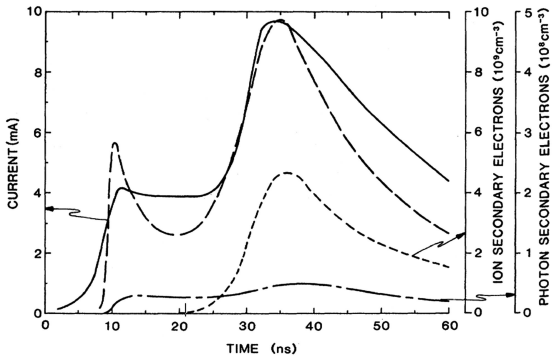


Fig. 2. Comparison of the computed and measured current waveform for the first pulse. And the computed number of secondary electrons due to photons and the number of secondary electrons due to ions.[23]

3.1.2. Ion-induced secondary electron emission

Ion-induced secondary electron emission (ISEE), the most common secondary electron emission mechanism, plays an important role in the later stage of Trichel pulse. It is slower than other fast mechanisms, such as photoemission,[20,23] field emission,[24] and streamer theory,[28] since the mobility of positive ions is low. And ISEE becomes predominant after more than a decade of nanoseconds according to simulations. Amin[20] and Morrow[23] proposed that ISEE was responsible for the plateau in the trailing edge and the second rising process in the stepped leading edge (Fig. 2), respectively (slower than photoemission). Paillol *et al.*[24,25] concluded that ISEE had a weak effect on the initial stage at high pressure (field emission dominates), as shown in Fig. 3. Many two-dimensional (2D) fluid models that were built to simulate the whole process of Trichel pulse successfully[31–38] only considered ISEE as the feedback mechanism. The flux of ISEE (Γ_e) is easy to calculate in the fluid models and determined by

$$\Gamma_e = -\gamma_i \Gamma_i, \tag{5}$$

where Γ_i is the flux of positive ion on the boundary, γ_i is the secondary emission factor (usually set as 0.001–0.01). The reason for choosing a proper value of γ_i is rarely clarified, while the sensitivity of γ_i has been discussed in some works. For example, as discovered by Sattari *et al.*,[37] when γ_i varies from 0.005 to 0.08, there is only a little impact on Trichel pulse characteristics. Other work by Tran *et al.*[38] shows that with γ_i increasing from 0.002 to 0.006, pulse peak, frequency, and averaged charge per pulse increase. Similar conclusions were also summarized in Ref. [39].

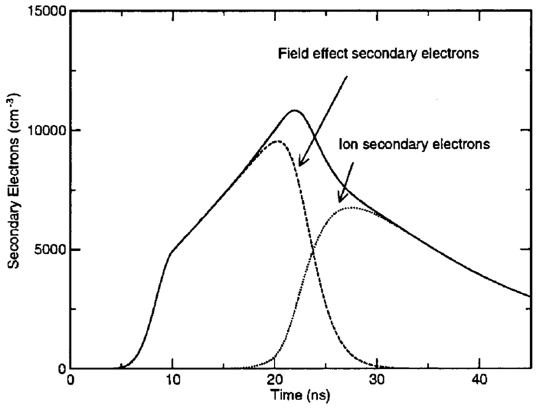


Fig. 3. The number of electrons emitted at the cathode surface. Field emission (solid line), ISEE (dotted line). From Ref. [25].

3.2. Field emission

Field emission is especially emphasized at high pressure, especially at atmospheric pressure. Because generating Trichel pulse at high pressure needs a higher electric field. When the electric field achieves about the order of 10^7 V/m–10^8 V/m, field emission will become significant with impurities on the surface.[25] Another reason is that photoemission maybe not applicable to the initial process at high pressure. For example, the leading edge at atmospheric pressure is on the order of nanoseconds, which is shorter than the

lifetime ($\sim$ 60 ns) of the excited states of nitrogen and oxygen molecules in the air. So that the photoemission caused by photons released from these excitation processes can be neglected.[24]

The field emission current density follows the Fowler–Nordheim relationship[57] and can be rewritten in Ref. [24],

$$j = B_1 \frac{E^2}{\Phi t^2(y)} \exp\left(-B_2 v(y) \frac{\Phi^{3/2}}{E}\right), \tag{6}$$

where $y = 3.79 \times 10^{-5}\sqrt{E}/\Phi$, E is the electric field value applied to the cathode, Φ is the work function of the cathode material in unit eV, $t(y)$ and $v(y)$ are special functions of the y variable,[57] B_1 and B_2 are two constants. And a field magnification factor β is often used for adjusting the electric field ($E = \beta E_0$) to coincide with the real value of the electric field on the cathode surface caused by impurities.[24] β can be time-dependent for modeling a sudden burst of electrons at the cathode.[25] In 2004, Paillol *et al.*[26] focused on another mechanism, space charge limited currents with Poole–Frenkel emission (SCLC+PF),[58] involving emission from an insulation layer,

$$j = AE^2 \exp(C\sqrt{E}), \tag{7}$$

where A and C are constants with respect to the electric field and are affected by the temperature and the insulator material. Then they investigated the field emission of a Mo needle cathode covered by an insulation layer because of handled in the air frequently. By applying SCLC+PF boundary condition, their simulation results agreed well with the experimental observation.

3.3. Streamer theory

Černák *et al.*[27,28,59,60] attributed the initial stage of the fast leading edge to the streamer theory for a wide range of conditions due to the propagation of the streamer being not affected by the electrons from the cathode. In Refs. [28,29], they summarized some experimental observations that were in contrast to the Townsend theory. For example, after coating the cathode with CuI or graphite (affect photoemission or ISEE), the change of current waveforms was not consistent with the prediction, *i.e.*, the insensitivity of the current waveforms to the cathode material. Then, to explain their results satisfactorily, they proposed the streamer mechanism occurring in a narrow layer in the vicinity of the cathode rather than through the whole gap. It begins with avalanches fed by cathode electrons emission (Townsend mechanism). After that, the space charge will accumulate in the space until its density is large enough to distort the Laplace electric field and leads to the appearance of both positive and negative streamers. The positive streamer moves toward the cathode and when it arrives at the cathode the current will reach the peak value. The streamer evolution process is independent of the cathode electron emission and the velocity is on the order of 10^8 cm/s,[28] which fully explains experiment results. This kind of streamer shares the same mechanism with a common streamer discharge,[61,62] so it is an example of "the unification of a wide scale of high-pressure gas discharges within the general class of positive streamer initiated breakdown phenomena".[29]

As this kind of streamer is an extremely fast process within a tiny region, optical observation is hard to be performed for a long time (so they named this theory as a hypothesis sometimes). Recently, some optical observations of the streamer were provided in some experiments by Hoder *et al.*[63–65] They used a set of spatiotemporal resolution optical diagnosis system, called time-correlated single photon counting technique (TC-SPC), to record the light intensity of molecular nitrogen at 337.1 nm (Second Positive System, SPS) and 391.5 nm (First Negative System, FNS) with the initiation processes of Trichel pulse in different distances from the cathode. In this way, they provided direct experimental optical evidence for streamer mechanism, as shown in Fig 4.[65] The positive streamer is ignited at $\sim$ 193 ns in $\sim$ 200 μm from the cathode and reaches the cathode at $\sim$ 195 ns. At the same time, a maximum FNS signal is created at the cathode surface, followed by the negative streamer starting in $\sim$ 200 μm–300 μm. The velocities of positive and negative streamers are 0.8×10^5 m/s and 1.7×10^5 m/s, respectively. This phenomenon is consistent with the theory put forward by Černák.

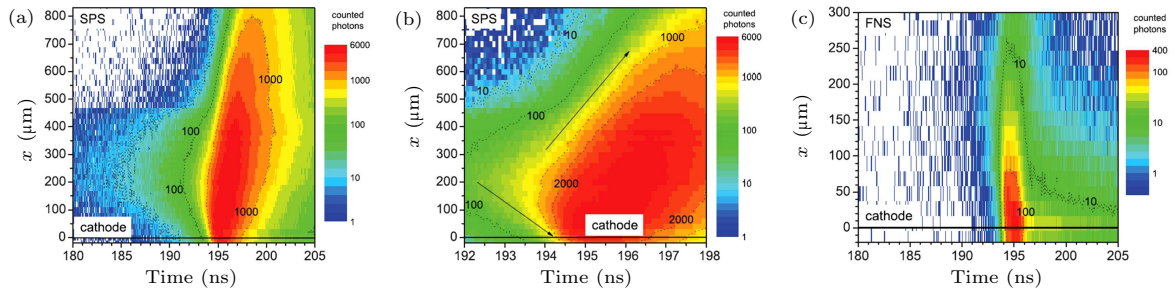


Fig. 4. 337.1 nm (a), 337.1 nm enlarged (b), and 391.5 nm (c) high-resolution TC-SPC recordings of the Trichel pulse breakdown for the setup of steel electrode with 240-μm curvature. The vertical axis (x) is the distance from the cathode. Reproduced from Ref. [65].

Photoionization is an essential mechanism to supply seed electrons for the propagation of positive streamers in air, where photoionization is caused by oxygen molecules absorbing photons emitted from excited nitrogen molecules. A few researchers[33,66,68] have simulated the impact of photoionization on Trichel pulse in air through similar 2D axisymmetric fluid models. In these models, the three-term exponential Helmholtz equations were solved to calculate the photoionization rate based on the theory of Bourdon.[69] The results demonstrate that the effect of photoionization on the Trichel pulse is not as significant as on positive streamers. For example, reference [68] reports that the number of electrons produced by the impact ionization is on average 100 times larger than photoionization.

4. Quenching mechanisms of Trichel pulse

A general concept of the quenching mechanism — negative ion forming near the cathode and suppressing the electric field — is widely accepted.[1] While with the development of simulations and experiments, more detailed processes have been further investigated. On the other hand, since the pulsed modes in non-electronegative gases[40–45] cannot be explained by the impact of negative ion, a lot of researchers have devoted to revealing its mechanisms. In this section, we will review some quenching mechanisms involving pulsed modes in both electronegative and non-electronegative gases respectively.

4.1. The quenching mechanisms in electronegative gases

The quenching process in electronegative gases can last for tens to hundreds of nanoseconds. At the initial quenching process, the dominant mechanism is caused by the accumulation and movement of the positive ions. Then with the development of discharge, the effect of the negative ions becomes obvious gradually.

4.1.1. Initial quenching process

A well-accepted work was provided by Morrow using a 1.5D fluid model to simulate the first Trichel pulse in oxygen at low pressure.[22] In order to judge the possibility of a self-sustained discharge occurring, he proposed a replenishment criterion (here shows a general form in Ref. [15]),

$$u_{\mathrm{r}} = \gamma \int_0^d \alpha \exp\left[\int_0^x (\alpha - \eta)\,\mathrm{d}x'\right]\mathrm{d}x, \tag{8}$$

where γ is the total secondary emission factor (In Morrow's paper, they only considered photoemission γ_{p}), α is the ionization coefficient, η is the attachment coefficient, d is the gap distance. If $u_{\mathrm{r}} \geq 1$, the self-sustained discharge will occur, while when $u_{\mathrm{r}} < 1$, the discharge will quench. Morrow divided the current waveform in a pulse into different phases shown in Fig. 5(a), and the electric field at different phases shown in Fig. 5(b). From phase A to phase D, with the development of the discharge, the positive ions accumulate and form the positive space charge gradually near the cathode. Then the positive space charge moves to the cathode slowly and forms a cathode sheath. The positive space charge will enhance the electric field between the cathode and itself, while weaken the electric field on the other side. At the same time a plasma will generate outside the sheath (Fig. 5(b) 0.02 cm $< x <$ 0.2 cm after 43 ns) where the electric field tends to zero, which reduces the ionization region. Finally, when the ionization region reduces to some extent leading to $u_{\mathrm{r}} < 1$, the discharge progressively quenches. Morrow views this process as the formation of a "transient cathode sheath". The whole process can be summarized as the electric field distortion due to positive ions accumulation and shrinking of the ionization region leads to discharge not sustaining further. This mechanism was also reported in other simulation results such as Refs. [24,25,32,38]. These works include results at different pressures, which means that this process is applicable at both low and high pressure.

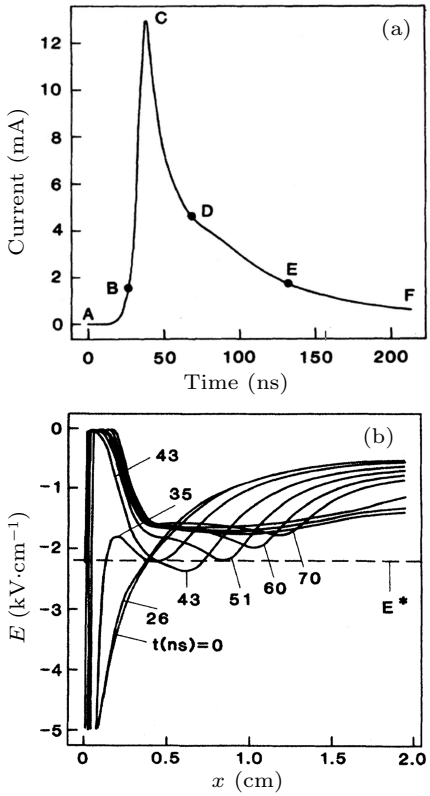


Fig. 5. The current waveform in a period and discharge phases (a), electric field along the gap at different times (the cathode at $x = 0$, the anode at $x = 2$ cm), E^* is the electric field at which $\alpha = \eta$ (b). Reproduced from Ref. [22].

4.1.2. Negative ion related mechanism

The role of negative ion is irreplaceable to the quenching process, especially after the initial quenching process. On one hand, the mobility of negative ions is much lower than that of electrons. According to Sato's equation,[70] the migration velocity of charged particles affects the current. So, after the

electrons convert to negative ions, the current will decrease. On the other hand, the accumulation of the negative ion near the cathode forms the negative space charge, which will lead to a reduction of the electric field between itself and the cathode. As a result, the ionization process is further weakened. The electric field recovers with the negative space charge migrating away from the cathode. The next pulse begins before the negative ions generated by the former pulses are clear from the gap, so there will be many negative ion "clouds" in the gap at the same time. This phenomenon is predicted by Lama *et al.*[30] and confirmed in many 2D simulations, such as Ref. [33] shown in Fig. 6.

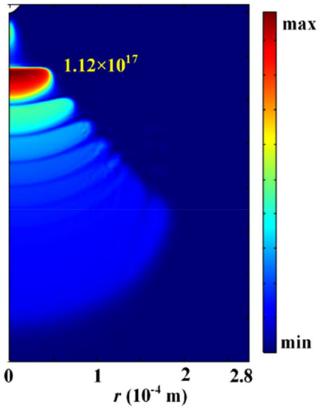


Fig. 6. Distribution of negative ions, we can distinguish different negative ion clouds generated by former pulses. Reproduced from Ref. [33].

In air or nitrogen/oxygen mixtures, lots of kinds of negative ions will be generated in Trichel pulse, among which O^- and O_2^- are two important initial negative ions.[22,71,72] O^- and O_2^- are generated through the dissociative attachment reaction (Eq. (9)) and three-body attachment reaction (Eq. (10)), respectively,[73]

$$e+O_2 \rightarrow O^- + O, \tag{9}$$

$$e+O_2+O_2 \rightarrow O_2^- + O_2. \tag{10}$$

The dissociative attachment reaction dominates in a high electric field region, while in a low electric field the three-body attachment reaction prevails (the criteria is related to electron energy ~ 1 eV).[74] Large parts of 2D fluid models only consider O_2^- to simulate the air at atmospheric pressure. While there are still some works that reveal their different roles in quenching Trichel pulse. Amin[20] proposed that the O^- was the major negative ion to reduce the electric field. Morrow[22] combined both reactions in his simulation model (oxygen at 50 Torr, 1 Torr = 1.3332×10^2 Pa) and emphasized the role of the three-body attachment in the trailing edge. Scott *et al.*[71] investigated that the quenching process became longer dramatically with the increase in the percentage of nitrogen from 0% to 80% at 20 Torr–100 Torr, which more likely is caused by O^- rather than O_2^- through some complex plasma chemical processes. Moreover, O^- and O_2^-, can convert to other negative ions depending on different conditions. Gardiner *et al.*[75] regarded that when considering CO_2 in the air the CO_3^- was dominant in the air at 10 Torr–30 Torr. Durán-Olivencia *et al.*[72] put forward that the dominant negative changes can be O^- or O_2^- during the pulse, O_2^- and O_3^- during the inter-pulse interval stage in oxygen at 50 Torr.

4.2. The quenching mechanisms in non-electronegative gases

As Raizer's textbook said, Trichel pulse was observed only in the electronegative gases[1] (such as air and SF_6[76,77]), but there have been quite lots of works about the negative DC pulsed mode in various non-electronegative gases.[28,40,42–45] Sun *et al.*[44] reported that the current waveforms within 30 ns were the same in both nitrogen and air at atmospheric pressure. A similar trend has been discussed involving the initial stage of the breakdown by Černák *et al.*[40] After comparing the initial stage of the breakdown current under negative DC voltage in nitrogen and the Trichel pulse current in electronegative gases, they found that the leading edge and the initial quenching process are quite similar. Morrow[22] found that the leading edge and the initial decay did not change dramatically after excluding the attachment reactions in his model. Akishev *et al.*[41,42] systematically investigated the pulsed mode in nitrogen and built a simulation model. They revealed that the initial quenching process is similar to the formation of a transient cathode sheath in electronegative gas. From these researches, we can conclude that the initial quenching mechanisms of both two kinds of gases are due to the same mechanism.

What is more, Ouyang *et al.*[43] put forward that the pulsed mode in various kinds of gases can be regarded as the mode transition from the low-current Townsend discharge to the high-current normal glow discharge, whose transition criterion is the positive ion flux (the flux difference of two modes can reach at least 2-order magnitude). And when the flux is between the two modes, the pulsed mode appears. They also reported the same mechanism of pulsed mode in other configurations.[78]

Besides the quenching mechanisms caused by the gas itself, some other researchers emphasized the profound role of the external circuit. Sun *et al.*[44] emphasized that in nitrogen the pulsed mode can be realized only with a large ballast resistor (MΩ), which leads the source to not supply charge in time, so the discharge is only fueled by the charge from the stray capacitance. Then the voltage of the stray capacitance, which equals cathode voltage, will drop until the discharge is quenched. Then the source will charge the stray capacitance again, and the discharge will restart when the cathode voltage raises to onset voltage. There might be a second hump appearing in the trailing edge due to the further development

of temporal glow discharge. Another equivalent circuit theory was discussed by Sigmond.[45] The ionization region ($\alpha > \eta$) is modeled by negative resistance (R_i), region capacitance (C_i), and discharge inductance (L_i), while the drift region ($\alpha < \eta$) modeled by equivalent resistance (R_d). R_d in electronegative gas is larger since the negative ion moves more slowly than electron. When R_d is large enough, the pulsed mode can appear. Otherwise, the external circuit resistance (R_0) and capacitance (C_0) will take over the role of R_d and C_i to make pulsed mode happen. The effect of negative ion and the resistor of the external circuit can be unified as a kind of impedance in this theory.

5. Conclusions

This review focuses on a classical discharge mode of negative DC corona in a nonuniform electric field, Trichel pulse. Many basic optical and electrical characteristics of it are present, and we discuss the well-accepted ionization and quenching mechanisms in detail. Ionization mechanisms mainly involve several electron emission mechanisms and streamer theory, whose applicability is identified at the same time. The positive ion and the negative ion related mechanism dominate different stages of the quenching process in electronegative gases. In non-electronegative gases positive ion dominates the initial quenching process too, while the effect of external circuit replaces the effect of negative ion.

Although different kinds of ionization and quenching mechanisms of Trichel pulse have been clarified, it is still far away from reaching a consensus. As an outlook, further simulations and experiments are required. Most present 2D models rarely consider the chemical process and various electron emission mechanisms, and simulations probably can play increasing roles in exploring the underlying mechanisms in different conditions. On the other hand, advanced diagnosis techniques are promoted in recent years, which can be effective methods in diagnosing the microscopic processes in Trichel pulse.

References

[1] Raizer Y P and Allen J E 1997 *Gas discharge physics* (Berlin: Springer) pp. 345–352
[2] Zhang B, Li Z and He J 2017 *Phys. Plasmas* **24** 103521
[3] Wang C, Chen X, Tang K and Li P 2019 *Plasma Sci. Technol.* **21** 055402
[4] Antao D S, Staack D A, Fridman A and Farouk B 2009 *Plasma Sources Sci. Technol.* **18** 035016
[5] Adamiak K 1994 *IEEE Trans. Ind. Appl.* **30** 381
[6] Alotto P and Codecasa L 2015 *IEEE Trans. Magn.* **52** 1
[7] Castle G S P 2001 *J. Electrost.* **51** 1
[8] Ghahfarokhi M S and Khayamian T 2011 *Rev. Sci. Instrum.* **82** 055114
[9] Mokhtari Z, Hole S and Lewiner J 2013 *J. Electrost.* **71** 769
[10] Kovalova Z, Zahoran M and Zahoranová A and Machala Z 2014 *J. Phys. D: Appl. Phys.* **47** 224014
[11] Chang J S, Lawless P A and Yamamoto T 1991 *IEEE Trans. Plasma Sci.* **19** 1152
[12] Ma S, Cheng H, Li J, Xu M, Liu D and Ostrikov K 2020 *Atmos. Chem. Phys.* **20** 11717
[13] Zhang Y, Cheng H, Gao H, Liu D and Lu X 2020 *High Volt.*
[14] Zhang T, Zhang Y, Ji Q, Li B and Ouyang J 2019 *Chin. Phys. B* **28** 075202
[15] Goldman M and Sigmond R S 1982 *IEEE Transactions on Electrical Insulation* **17** 90
[16] Akishev Y, Grushin M, Kochetov I, Karal'Nik V, Napartovich A and Trushkin N 2005 *Plasma Sources Sci. Technol.* **14** S18
[17] Trichel G W 1938 *Phys. Rev.* **54** 1078
[18] Loeb L B 1948 *J. Appl. Phys.* **19** 882
[19] Loeb L B 1952 *Phys. Rev.* **86** 256
[20] Amin M R 1954 *J. Appl. Phys.* **25** 627
[21] Aleksandrov G N 1963 *Soviet Physics-Technical Physics* **8** 161
[22] Morrow R 1985 *Phys. Rev. A* **32** 1799
[23] Morrow R 1985 *Phys. Rev. A* **32** 3821
[24] Reess T and Paillol J 1997 *J. Phys. D: Appl. Phys.* **30** 3115
[25] Paillol J, Espel P, Reess T, Gibert A, and Domens P 2002 *J. Appl. Phys.* **91** 5614
[26] Bessieres D, Paillol J and Soulem N 2004 *J. Appl. Phys.* **95** 3943
[27] Černák M, Hosokawa T and Odrobina I 1993 *J. Phys. D: Appl. Phys.* **26** 607
[28] Černák M, Hosokawa T, Kobayashi S and Kaneda T 1998 *J. Appl. Phys.* **83** 5678
[29] Černák M, Hoder T and Bonaventura Z 2020 *Plasma Sources Sci. Technol.* **29** 013001
[30] Lama W L and Gallo C F 1974 *J. Appl. Phys.* **45** 103
[31] Deng F C, Ye L Y and Song K C 2013 *J. Phys. D: Appl. Phys.* **46** 425202
[32] Dordizadeh P, Adamiak K and Castle G S P 2015 *J. Phys. D: Appl. Phys.* **48** 415203
[33] Zheng Y, Wang L, Wang D and Jia S 2017 *Phys. Plasmas* **24** 063515
[34] Xia Q, Zhang Y, Jiang Z, Wang R and Ouyang J 2017 *J. Phys. D: Appl. Phys.* **50** 505205
[35] Chen S, Li K and Nijdam S 2019 *Plasma Sources Sci. Technol.* **28** 055017
[36] Lu B, Feng Q and Sun H 2018 *IEEE Trans. Plasma Sci.* **47** 149
[37] Sattari P, Gallo C F, Castle G S P and Adamiak K 2011 *J. Phys. D: Appl. Phys.* **44** 155502
[38] Tran T N, Golosnoy I O, Lewin P L and Georghiou G E 2010 *J. Phys. D: Appl. Phys.* **44** 015203
[39] Dordizadeh P, Adamiak K and Castle G S P 2016 *J. Electrost.* **84** 73
[40] Černák M and Hosokawa T 1988 *Appl. Phys. Lett.* **52** 185
[41] Akishev Y S, Grushin M E, Karal'Nik V B and Trushkin N I 2001 *Plasma Phys. Rep.* **27** 520
[42] Akishev Y S, Grushin M E, Karal'Nik V B and Trushkin N I 2001 *Plasma Phys. Rep.* **27** 532
[43] Zhang Y, Xia Q, Jiang Z and Ouyang J 2017 *Sci. Rep.* **7** 10135
[44] Zhang X, Guo Y, Sun A, Yao C, Sun G and Zhang G 2020 *Phys. Plasmas* **27** 033501
[45] Sigmond R S 1996 *AIP Conf. Proc.* **363** 332
[46] Chen S, van den Berg R G W and Nijdam S 2018 *Plasma Sources Sci. Technol.* **27** 055021
[47] Zhang Y, Qin Y, Zhao G and Ouyang J 2016 *J. Phys. D: Appl. Phys.* **49** 245206
[48] Greenwood A 1952 *J. Appl. Phys.* **23** 1316
[49] Amirov R H, Barengolts S A, Korostylev E V, Pestovskii N V, Petrov A A, Samoylov I S and Savinov S Y 2014 *J. Phys.: Conf. Ser.* **550** 012052
[50] Liu L and Becerra M 2017 *J. Phys. D: Appl. Phys.* **50** 105204
[51] Townsend J S 1915 *Electricity in gases* (Oxford: Clarendon Press) pp. 377–378
[52] Yamada K 2004 *J. Appl. Phys.* **96** 2472
[53] Ferreira G F L, Oliveira Jr O N and Giacometti J A 1986 *J. Appl. Phys.* **59** 3045
[54] Meng X, Zhang H and Zhu J 2008 *J. Phys. D: Appl. Phys.* **41** 065209
[55] Li Z, Zhang B and He J 2013 *Phys. Plasmas* **20** 093507
[56] Li Z, Zhang B, He J and Xu Y 2014 *Phys. Plasmas* **21** 012113
[57] Fowler R H and Nordheim L 1928 *Proceedings of the Royal Society of London. Series A, Containing Papers of a Mathematical and Physical Character* **119** 173
[58] May P W, Höhn S, Ashfold M N, Wang W N, Fox N A, Davis T J and Steeds J W 1998 *J. Appl. Phys.* **84** 1618

[59] Zahoranová A, Kúdelcík J, Paillol J and Černák M 2002 *J. Phys. D: Appl. Phys.* **35** 762
[60] Kúdelčík J, Zahoranová A, Halanda J and Černák M 2014 *J. Electrost.* **72** 417
[61] Li H, Sun A, Zhang X, Yao C, Chang Z and Zhang G 2018 *Acta Phys. Sin.* **67** 045101 (in Chinese)
[62] Sun A, Teunissen J and Ebert U 2014 *J. Phys. D: Appl. Phys.* **47** 445205
[63] Hoder T, Černák M, Paillol J, Loffhagen D and Brandenburg R 2012 *Phys. Rev. E* **86** 055401
[64] Hoder T, Bonaventura Z, Bourdon A and Šimek M 2015 *J. Appl. Phys.* **117** 073302
[65] Hoder T, Loffhagen D, Voráč J, Becker M M and Brandenburg R 2016 *Plasma Sources Sci. Technol.* **25** 025017
[66] Lu B X and Sun H Y 2016 *AIP Adv.* **6** 095111
[67] Sun H Y, Lu B X, Wang M, Guo Q F and Feng Q K 2017 *Phys. Plasmas* **24** 103506
[68] Dordizadeh P, Adamiak K and Castle G S P 2016 *Plasma Sources Sci. Technol.* **25** 065009
[69] Bourdon A, Pasko V P, Liu N Y, Célestin S, Ségur P and Marode E 2007 *Plasma Sources Sci. Technol.* **16** 656
[70] Morrow R and Sato N 1999 *J. Phys. D: Appl. Phys.* **32** L20
[71] Scott D A and Haddad G N 1987 *J. Phys. D: Appl. Phys.* **20** 1039
[72] Durán-Olivencia F J, Pontiga F and Castellanos A 2014 *J. Phys. D: Appl. Phys.* **47** 415203
[73] Skalny J D, Mikoviny T, Matejcik S and Mason N J 2004 *Int. J. Mass Spectrom.* **233** 317
[74] Gravendeel B and De Hoog F J 1987 *J. Phys. B: At. Mol. Opt. Phys.* **20** 6337
[75] Gardiner P S and Craggs J D 1977 *J. Phys. D: Appl. Phys.* **10** 1003
[76] He Y, Sun A, Xue J, Shen Z, Zhang X and Zhang G 2020 *AIP Adv.* **10** 055027
[77] He Y, Sun A, Zhang X, Xue J and Zhang G 2020 *AIP Adv.* **10** 085303
[78] Xia Q, Zhang Y, He F, Qin Y, Jiang Z and Ouyang J 2018 *Phys. Plasmas* **25** 023506